Numerische Mathematik
https://doi.org/10.1007/s00211-024-01395-x

Numerische Mathematik

Wave scattering problems in exterior domains with the method of fundamental solutions

Carlos J. S. Alves[1] · **Pedro R. S. Antunes**[2]

Received: 10 December 2021 / Revised: 29 July 2023 / Accepted: 21 January 2024

Abstract
The method of fundamental solutions has been mainly applied to wave scattering problems in bounded domains and to our knowledge there have not been works addressing density results for general shapes, or addressing the calculation of the complex resonance frequencies that occur in exterior problems. We prove density and convergence of the fundamental solutions approximation in the context of wave scattering problems, with and without a priori knowledge of the frequency, which is of particular importance to detect resonance frequencies for trapping domains. We also present several numerical results that illustrate the good performance of the method in the calculation of complex resonance frequencies for trapping and non trapping domains in 2D and 3D.

Mathematics Subject Classification 65N35 · 65N80 · 35J05

1 Introduction

Problems of scattering of time-harmonic acoustic waves by obstacles have a lot of physical applications. Probably some of the most effective numerical methods for the solution of these problems belong to the class of boundary integral equations methods, where the solution is represented in terms of boundary layers defined on some

P.R.S.A. was partially supported by FCT, Portugal, through the scientific project UIDB/00208/2020.

✉ Pedro R. S. Antunes
prsantunes@tecnico.ulisboa.pt

Carlos J. S. Alves
carlos.alves@math.tecnico.ulisboa.pt

[1] Departamento de Matemática and CEMAT, Instituto Superior Técnico, Av. Rovisco Pais 1, 1049-001 Lisboa, Portugal

[2] Departamento de Matemática and Grupo de Física Matemática, Instituto Superior Técnico, Av. Rovisco Pais 1, 1049-001 Lisboa, Portugal

Published online: 28 February 2024

hypersurface S. These methods provide solutions satisfying the partial differential equation in the whole (unbounded) region where the wave propagation occurs and reduce the problem to the solution of integral equations defined on S. Moreover, the radiation condition at infinity is also satisfied, provided a convenient fundamental solution is chosen. However, this kind of methods suffer from the existence of irregular frequencies that correspond to characteristic wave numbers associated to an interior eigenvalue problem. For these spurious eigenfrequencies the integral equation looses uniqueness of solution and thus, the linear system obtained from the discretization of the integral equation is extremely ill-conditioned.

Several techniques have been addressed to tackle the problem of irregular frequencies in boundary integral methods. For instance, approaches using representations by a mixed potential, involving single layer and double layer potentials [11, 24] revealed to provide a unique solution for all wavenumbers. Another possibility is to use the combined Helmholtz interior integral equation formulation [12, 26, 27], where some interior points are placed allowing to define additional equations in order to produce the constraints needed to have a unique solution of the integral equation.

In this work we will study the application of the method of fundamental solutions (MFS) for the solution of scattering problems. The MFS has been widely used for solving to interior problems [2, 4, 5, 8, 10, 13, 18, 29] and its application to a radiation problem was considered in [15]. However, we are not aware of previous works addressing density results for general shapes, or considering the solution of the resonance problem with unbounded regions.

The resonance frequencies or scattering resonances are generalized eigenfrequencies or bound states for which the energy can scatter to infinity. It can be proven that they are complex numbers with negative imaginary part, where essentially, the real part of the resonance frequency defines the rate of oscillation associated to the bound state while the imaginary part determines the rate of decay.

The distribution of the resonances in the complex plane has a strong connection with the geometry of the scatterer. In particular, the study of the billiard flow defined by the propagation of a straight line with perfect reflection at the boundary allows to classify the domains as trapping or non trapping, depending wether there exists trajectories of the billiard flow that never escape to infinity. The resonances of non trapping domains move away from the real axis when we consider resonance frequencies with increasing real part, while for trapping domains it is always possible to find some resonance frequencies arbitrarily close to the real axis, provided we take a range of frequencies with sufficiently large real part [3, 6, 7, 16, 19–21, 23, 25]. In Sect. 6, we will present some numerical results for the location of the resonance frequencies of some trapping and non trapping domains.

The paper is organized as follows. In Sect. 2 we introduce the scattering problem and a numerical approach to this problem using the method of fundamental solutions is described in Sect. 3. We devote Sect. 4 to address density and convergence results supporting the application of the method in the context of scattering problems. In Sect. 5 we introduce the resonance problem and present some classical results for the distribution of the resonance frequencies in the complex plane for trapping and non trapping domains. Section 6 presents some numerical tests and simulations for 2D and 3D trapping and non trapping domains and finally, Sect. 7 contains some conclusions.

2 Wave scattering problems

We consider the time-harmonic scattering problem in the range of resonance frequencies. Let $\Omega \subset \mathbb{R}^D$ be a bounded domain, in dimension $D = 2$ or 3, also called an *obstacle*, which scatters an acoustic incident plane wave, for instance, of the form

$$u^{inc}(x) = e^{ikx\cdot d}, \tag{2.1}$$

where $d \in \mathbb{R}^D$ with $|d| = 1$ determines the direction of propagation of the incident acoustic wave. The obstacle Ω might be a simply connected shape or the union of several simply connected shapes. In that case we take $\Omega = \Omega_1 \cup ... \cup \Omega_C$ where C stands for the number of simply connected components. We will also use a similar notation for the boundary and its parts:

$$\Gamma = \partial\Omega = \partial\Omega_1 \cup ... \cup \partial\Omega_C = \Gamma_1 \cup ... \cup \Gamma_C. \tag{2.2}$$

For a given wavenumber $\kappa \in \mathbb{R}$, the scattered wave u satisfies the Helmholtz equation, and we consider the exterior problem

$$\begin{cases} \Delta u + \kappa^2 u = 0 & \text{in } \mathbb{R}^D \backslash \bar{\Omega} \\ \mathscr{B}u = -\mathscr{B}u^{inc} & \text{on } \Gamma \\ \partial_r u - i\kappa u = o(r^{(1-D)/2}) \text{ when } r = |x| \to \infty \end{cases} \tag{2.3}$$

where the last condition is the Sommerfeld radiation condition.

The boundary condition is defined by an operator $\mathscr{B}$ which might be the trace operator, in the case of a Dirichlet boundary condition, or the normal derivative in the case of a Neumann boundary condition.

It is well known that this problem is well posed (e.g. [14]) and that the behavior of the scattered wave can be described by the asymptotic relation

$$u(x) = \frac{e^{ikr}}{r^{(D-1)/2}} u_\infty(\hat{x}) + o\left(\frac{1}{r}\right) \tag{2.4}$$

where $\hat{x} = \frac{x}{|x|}$ and u_∞ is the *far field pattern*, an analytic function with complex values, defined on the unitary circle/sphere $S = \{x \in \mathbb{R}^D : |x| = 1\}$.

3 Method of fundamental solutions

We will make use of the fundamental solution for the Helmholtz operator, which is given by the Hankel function in 2D,

$$\Phi(r) = \frac{i}{4} H_0^{(1)}(\kappa r) \quad \text{with } H_0^{(1)} = J_0 + iY_0, \tag{3.1}$$

with $r = |x|$, and in 3D is given by

$$\Phi(r) = \frac{\exp(i\kappa r)}{4\pi r}. \tag{3.2}$$

In both cases, these fundamental solutions verify the Sommerfeld radiation condition.

Thus, with any $y \in \Omega$, the point sources, which are shifted fundamental solutions $\phi_y(\cdot) = \Phi(\cdot - y)$ verify

$$\begin{cases} \Delta\phi_y + \kappa^2\phi_y = 0 & \text{in } \mathbb{R}^D \backslash \bar{\Omega} \\ \partial_r\phi_y - i\kappa\phi_y = o(r^{(1-D)/2}) & \text{when } r = |x| \to \infty \end{cases} \tag{3.3}$$

and the only remaining condition to be satisfied in (2.3) is the boundary condition. It is then natural to consider a combination of point sources $y_1, \ldots, y_M \in \Omega$,

$$\tilde{u} = \sum_{m=0}^{M} \alpha_m \phi_{y_m} \tag{3.4}$$

such that $\mathscr{B}\tilde{u} = -\mathscr{B}u^{inc}$ on a set of collocation points $x_1, ..., x_N \in \Gamma$, usually taking $N \geq M$.

With the method of fundamental solutions this leads to the linear system

$$[\mathscr{B}\Phi(|x_n - y_m|)]\,[\alpha_m] = \left[-\mathscr{B}u^{inc}(x_n)\right], \tag{3.5}$$

and by the well posedness of the direct problem, we may control the approximation error by the difference on the boundary.

However, when $N = M$ and $\mathscr{B}$ is the identity, the matrix might be the transpose of the one we have for an associated interior problem.

More precisely suppose that we consider an open subset ω such that $\bar{\omega} \subset \Omega$, and then take its boundary $\gamma = \partial\omega$ to be the artificial set where the point sources are to be located (in the case of multiple components, $\gamma = \gamma_1 \cup ... \cup \gamma_C$).

Now for the Dirichlet problem we have the MFS system

$$[\Phi(|x_n - y_m|)]\,[\alpha_m] = \left[-u^{inc}(x_n)\right]. \tag{3.6}$$

But when the MFS is applied to the associated interior problem

$$\begin{cases} \Delta u + \kappa^2 u = 0 \text{ in } \omega \\ u = -u^{inc} \quad \text{on } \gamma \end{cases} \tag{3.7}$$

this leads to the system $[\Phi(|y_n - x_m|)]\,[a_m] = \left[-u^{inc}(y_n)\right]$, and the matrix is exactly the transposed one.

However in the interior problem there are eigenfrequencies associated to the domain ω and these frequencies may influence the results.

In fact, suppose that $-\kappa^2$ is a Laplace-Dirichlet eigenvalue, then the matrix is not invertible or extremely ill-conditioned for the interior problem, but this should not be the case for the exterior problem, where only complex eigenfrequencies exist.

We may try to reduce the dimension of the artificial domain ω such that the eigenvalues become higher in modulus than κ^2, but this will lead to poor results in the MFS since γ will not be sufficiently close to Γ to perform a good approximation of u^{inc}.

4 Density and convergence results

In this section we prove density and convergence results supporting the application of the method of fundamental solutions to solve scattering problems in exterior domains. In the first result we assume that the source set for the MFS is γ, the boundary of a bounded open set ω such that $\bar{\omega} \subset \Omega$ which is the most typical setting for the MFS. In this case, we will also assume that $-\kappa^2$ is not a Laplace-Dirichlet eigenvalue for the domain ω which implies well posedness of the interior problem defined in ω.

Theorem 1 *Let $\kappa \in \mathbb{C}$, $\bar{\omega} \subset \Omega$ and consider $\gamma = \partial\omega$. Assume that $-\kappa^2$ is not a Laplace-Dirichlet eigenvalue for the domain ω. Then*

$$\mathscr{S}_\gamma = span\left\{\phi_y : \ y \in \gamma\right\} \tag{4.1}$$

is dense in $H^{1/2}(\Gamma)$.

Proof Given any $\psi \in H^{-1/2}(\Gamma)$, we define the boundary single layer potential

$$u(y) = \left\langle \phi_y, \psi \right\rangle_{H^{1/2}(\Gamma)\times H^{-1/2}(\Gamma)} = \int_\Gamma \Phi(|y-x|)\psi(x)ds_x \tag{4.2}$$

and assume that $u(y) = 0$ for all $y \in \gamma$. By proving that $\psi \equiv 0$ the completeness follows from the orthogonality in dual Banach spaces, recalling that $H^{1/2}(\Gamma)$ is the dual space of $H^{-1/2}(\Gamma)$, using $L^2(\Gamma)$ as pivot space.

Since $-\kappa^2$ is not an eigenvalue associated to ω, the function u verifies the well posed interior problem

$$\begin{cases} \Delta u + \kappa^2 u = 0 \ \text{in } \omega \\ \quad u = 0 \qquad \text{on } \gamma \end{cases} \tag{4.3}$$

and we conclude that $u \equiv 0$ in ω. Since the function u is analytic in Ω (in fact, it is only singular on Γ) it is extended by zero to the boundary. Since the single layer potential is continuous through Γ we have $u = 0$ on Γ (e.g. [14]) and both inner and outer traces are null on Γ. This implies that u also verifies the homogeneous exterior problem

$$\begin{cases} \Delta u + \kappa^2 u = 0 & \text{in } \mathbb{R}^D \backslash \bar{\Omega} \\ u = 0 & \text{on } \Gamma \\ \partial_r u - i\kappa u = o(r^{(1-D)/2}) & \text{when } r = |x| \to \infty \end{cases} \tag{4.4}$$

which is well posed and the unique solution is zero. Thus we conclude that $\psi = [\partial_\nu u] = 0$. □

We can drop the hypothesis in Theorem 1 that $-\kappa^2$ is not a Laplace-Dirichlet eigenvalue for the domain ω under an additional assumption that can be defined through the following definition.

Definition 1 We say that a set $S_\kappa \subset \bar{\omega}$ is a density source set for the MFS if the problem

$$\begin{cases} \Delta u + \kappa^2 u = 0 & \text{in } \omega \\ u = 0 & \text{on } \gamma \\ u = 0 & \text{in } S_\kappa \end{cases} \tag{4.5}$$

has a unique solution defined in $\bar{\omega}$, $u \equiv 0$.

And immediately we have the following result.

Corollary 1 *Let S_κ be a density source set for the MFS. Then*

$$\mathscr{S}_{S_\kappa} = span\left\{\phi_y : \ y \in S_\kappa\right\} \tag{4.6}$$

is dense in $H^{1/2}(\Gamma)$.

Proof The proof follows the same steps as the proof of Theorem 1 and we can conclude that $u \equiv 0$ in ω because S_κ is a density source set for the MFS. In this case we do not need to ensure that $-\kappa^2$ is not an eigenvalue. □

Now, we prove the following

Lemma 1 *Given $z, w \in \mathbb{R}^D \setminus \{0\}$ we have*

$$\left|\frac{z}{|z|} - \frac{w}{|w|}\right| \leq \frac{|z-w|}{\sqrt{|z||w|}}$$

Proof We have

$$|z-w|^2 = |z|^2 + |w|^2 - 2z\cdot w \Rightarrow -2z\cdot w = |z-w|^2 - |z|^2 - |w|^2 .$$

On the other hand,

$$\begin{aligned} \left|\frac{z}{|z|} - \frac{w}{|w|}\right|^2 &= \frac{|z|^2}{|z|^2} + \frac{|w|^2}{|w|^2} - \frac{2z\cdot w}{|z||w|} \\ &= 2 - \frac{2z\cdot w}{|z||w|} = \frac{2|z||w| + |z-w|^2 - |z|^2 - |w|^2}{|z||w|} \\ &= \frac{|z-w|^2 - (|z|-|w|)^2}{|z||w|} \leq \frac{|z-w|^2}{|z||w|} \end{aligned}$$

and the conclusion follows. □

Given a curve γ, we build a family of sets of points $\Gamma_M \subset \gamma$ defined by

$$\Gamma_1 = \{x_1\}, \quad \text{for some } x_1 \in \gamma$$

and

$$\Gamma_M = \Gamma_{M-1} \cup \{y : y \in \gamma \backslash \Gamma_{M-1}\}, \ M = 2, 3, ...$$

and say that a family Γ_M is dense in γ if

$$\forall_{\epsilon>0} \exists_{M\in\mathbb{N}} \forall_{x\in\gamma} \exists_{y\in\Gamma_M} : |y - x| < \epsilon.$$

Theorem 2 (Convergence with fundamental solutions) Let $\bar{\omega} \subset \Omega$ and $\gamma = \partial\omega$. Assume that $-\kappa^2$ is not a Laplace-Dirichlet eigenvalue for the domain ω. Consider a family of sets of points

$$\Gamma_M = \{y_1, \cdots, y_M\} \subset \gamma$$

which is dense in γ. Then, for any given $\varepsilon > 0$ and any $g \in H^{1/2}(\Gamma)$, there exists $M \in \mathbb{N}$, such that the error of

$$v_M(x) := \sum_{j=1}^{M} \alpha_j \Phi(|x - y_j|), \ y_j \in \Gamma_M \tag{4.7}$$

is bounded by ε, that is,

$$||g - v_M||_{H^{1/2}(\Gamma)} < \varepsilon. \tag{4.8}$$

Proof From the density result (Theorem 1), given $g \in H^{1/2}(\Gamma)$ we have an approximation $u_M \in \mathscr{S}_\gamma$,

$$u_M(x) = \sum_{j=1}^{M} \alpha_j \Phi(|x - s_j|) \tag{4.9}$$

such that $||u - u_M||_{H^{1/2}(\Gamma)} < \frac{\varepsilon}{2}$, for some $s_1, ..., s_M \in \gamma$ and some $\alpha_1, ..., \alpha_M \in \mathbb{C}$. Consider now

$$A = \sum_{j=1}^{M} |\alpha_j|, \quad F = \max_{r\in[r_0,r_1]} |\partial_r \Phi(r)| \quad \text{and} \quad G = \max_{r\in[r_0,r_1]} |\nabla\partial_r \Phi(r)|,$$

where

$$r_0 = \min_{x\in\Gamma, y\in\gamma} |x - y|, \quad r_1 = \max_{x\in\Gamma, y\in\gamma} |x - y|,$$

noticing that F and G are bounded, because $r_0 = dist(\Gamma, \gamma) > 0$.

Given any $\delta > 0$ and sufficiently large M, we have points in Γ_M sufficiently close to each of the source points s_j since Γ_M is dense in γ. Therefore,

$$|\Phi(|x - s_j|) - \Phi(|x - y_j|)| \leq ||\partial_r \Phi||_\infty |y_j - s_j| < F\delta.$$

Using Lemma 1 we have

$$\left| \frac{x - y_j}{|x - y_j|} - \frac{x - s_j}{|x - s_j|} \right| \leq \frac{|y_j - s_j|}{r_0}$$

and thus,

$$\begin{aligned}
|\nabla\Phi(|x - s_j|) - \nabla\Phi(|x - y_j|)| &= \left| \frac{x - s_j}{|x - s_j|} \partial_r \Phi(|x - s_j|) - \frac{x - y_j}{|x - y_j|} \partial_r \Phi(|x - y_j|) \right| \\
&= \left| \frac{x - s_j}{|x - s_j|} \left(\partial_r \Phi(|x - s_j|) - \partial_r \Phi(|x - y_j|) \right) \right. \\
&\quad \left. - \left(\frac{x - y_j}{|x - y_j|} - \frac{x - s_j}{|x - s_j|} \right) \partial_r \Phi(|x - y_j|) \right| \\
&\leq \left| \partial_r \Phi(|x - s_j|) - \partial_r \Phi(|x - y_j|) \right| \\
&\quad + \frac{|y_j - s_j|}{r_0} \left| \partial_r \Phi(|x - y_j|) \right| \\
&\leq ||\nabla \partial_r \Phi||_\infty |y_j - s_j| + \frac{||\partial_r \Phi||_\infty}{r_0} |y_j - s_j| \\
&= \left(||\nabla \partial_r \Phi||_\infty + \frac{||\partial_r \Phi||_\infty}{r_0} \right) |y_j - s_j| < \left(G + \frac{F}{r_0} \right) \delta.
\end{aligned}$$

Thus, by taking $v_M(x) = \sum_{j=1}^M \alpha_j \Phi(x - y_j)$ we get

$$|u_M(x) - v_M(x)| = \left| \sum_{j=1}^M \alpha_j \left(\Phi(|x - s_j|) - \Phi(|x - y_j|) \right) \right| < \sum_{j=1}^M |\alpha_j| F\delta = FA\delta.$$

and

$$\begin{aligned}
|\nabla u_M(x) - \nabla v_M(x)| &= \left| \sum_{j=1}^M \alpha_j \left(\nabla\Phi(|x - s_j|) - \nabla\Phi(|x - y_j|) \right) \right| \\
&< \sum_{j=1}^M |\alpha_j| \left(G + \frac{F}{r_0} \right) \delta = \left(G + \frac{F}{r_0} \right) A\delta.
\end{aligned}$$

Since δ is arbitrarily small, the approximation v_M is close enough to u_M such that $||u_M - v_M||_{H^{1/2}(\Gamma)} < \frac{\varepsilon}{2}$. The result follows from

$$||u - v_M||_{H^{1/2}(\Gamma)} \leq ||u - u_M||_{H^{1/2}(\Gamma)} + ||u_M - v_M||_{H^{1/2}(\Gamma)} < \varepsilon.$$

□

Remark 1 It is important to notice that the source points in Γ_M must be arbitrarily close to the source points $s_1, ..., s_M$ because the coefficients $\alpha_1, ..., \alpha_M$ might be arbitrarily large. In fact there is no bound for these coefficients, as this might be linked to an inversion of a compact operator.

This problem is linked to the inversion of the single layer potential $\mathscr{L}_\gamma$, since

$$(\mathscr{L}_\gamma \psi)(x) = \int_\gamma \Phi(|x - y|)\psi(y)ds_y = g(x) \quad \text{with } x \in \Gamma.$$

It is well known that $\mathscr{L}_\gamma : L^2(\Gamma) \to L^2(\Gamma)$ is a compact operator, and its inversion can only be achieved with regularization techniques, such as the Tikhonov regularization.

Corollary 2 *The same convergence result holds by taking source points in such a way that when $M \to \infty$, the set of source points is dense in a density source set for the MFS, with no restriction on κ.*

Proof It follows the same steps of the proof of Theorem 2, using Corollary 1 instead of Theorem 1. □

In brief, by Theorem 2 we conclude the method of fundamental solutions is convergent, provided $-\kappa^2$ is not a Laplace-Dirichlet eigenvalue for the domain ω. We can also prove convergence of the method without any assumption on the frequency κ, by Corollary 2, but in that case we must ensure that the set of source points is chosen in such a way that it is dense in a density source set for the MFS. One possibility is to take $S_\kappa \equiv \bar{\omega}$ which is (trivially) a density source set for the MFS. In that case, we shall locate the source points uniformly distributed in $\bar{\omega}$ in such a way that for any $\epsilon > 0$ and any point $\bar{y} \in \bar{\omega}$ there exists a (sufficiently large) M and a source point y_p such that $|\bar{y} - y_p| < \epsilon$.

Another possibility would be to take the source points in a density source set for the MFS that do not coincide with $\bar{\omega}$. We could think that by taking a few extra points z_k, for instance randomly chosen in ω, this could force the solution to be null, but this is not the case, as the eigenfunctions may present nodal sets. Thus, these eigenfunctions would also verify $u(z_k) = 0$ and this would not imply $u \equiv 0$ in ω. Therefore, the set of the points z_k chosen in this way might not be a density source set for the MFS. The same problem would occur using extra inner contours such as γ, as these contours might match a nodal set. Indeed, it is straightforward to see that for some choices of ω, we can verify that for any point $\bar{y} \in \omega$, there is an eigenfunction u of ω such that $\bar{y}$ is on a nodal line of u. For instance taking ω to be a disk, we know that some of the eigenvalues of ω have multiplicity two. This means that the dimension of the eigenspace is two and we have two linearly independent eigenfunctions associated with the same eigenvalue. In that case, we can tune the coefficients of a linear combination of these two eigenfunctions in order to build an eigenfunction that vanishes at the point $\bar{y}$. We can expect to be able to use the same type of construction for an arbitrary

region ω, provided some of the Dirichlet eigenvalues of ω are not simple. However, generically with respect to the domain, all the eigenvalues are simple in the sense that for any given planar domain there exists a small deformation of its boundary for which the eigenvalue of the deformed domain is simple (eg. [1, 22, 28]).

Typically we fix the range of frequencies for which we study solutions of the scattering problem. In that case, there is a finite number of eigenvalues of ω in that range of frequencies. In practice, we expect that a set S of sufficiently many random points uniformly distributed in ω can be used as a density source set for the MFS, in the sense that we expect that there is not an eigenfunction associated to an eigenvalue in that range of frequencies that vanish at all the points in S.

5 Resonance problem

Although there are no real resonance frequencies for the exterior acoustic problem with the Sommerfeld radiation condition, these frequencies exist in the complex form. However, in the complex case, the asymptotic condition must be extended, to include the asymptotic behavior of the fundamental solutions. For instance, in the 3D case, a solution given by the single layer potential verifies

$$u(x) = \int_\Gamma \Phi(|x-y|)\psi(y)ds_y = \exp(-\kappa_I r)O\left(\frac{1}{r}\right)$$

where $\kappa = \kappa_R + i\kappa_I$.

Thus, the Sommerfeld radiation is modified to include this asymptotic behavior, and the exterior problem is formulated for any $\kappa \in \mathbb{C}$

$$\begin{cases} \Delta u + \kappa^2 u = 0 & \text{in } \mathbb{R}^D \backslash \bar{\Omega} \\ \mathscr{B}u = -\mathscr{B}u^{inc} & \text{on } \Gamma \\ \partial_r u - i\kappa u = e^{-\kappa_I r} o(r^{(1-D)/2}) & \text{when } r = |x| \to \infty \end{cases} \tag{5.1}$$

We will look for the resonance frequencies $\kappa \in \mathbb{C}$ for which the problem (5.1) does not have an unique solution. In particular, we shall determine the frequencies κ for which the problem

$$\begin{cases} \Delta u + \kappa^2 u = 0 & \text{in } \mathbb{R}^D \backslash \bar{\Omega} \\ \mathscr{B}u = 0 & \text{on } \Gamma \\ \partial_r u - i\kappa u = e^{-\kappa_I r} o(r^{(1-D)/2}) & \text{when } r = |x| \to \infty \end{cases} \tag{5.2}$$

has a nontrivial solution.

5.1 Trapping and non trapping domains

We start by introducing some definitions which allow to classify each domain as trapping or non trapping.

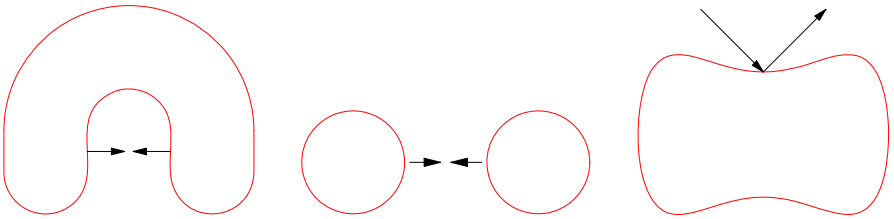

Fig. 1 Examples of two trapping domains and a non trapping domain (respectively)

Definition 2 (*Geometric optics reflection*) Given a pair (x_0, v_0) where $x_0 \in \mathbb{R}^D \backslash \Omega$ is a point and $v_0 \in S^{D-1}$ is a unitary vector, we will consider the half line $\rho^+_{(x_0,v)} = \{x_0 + t v_0 : t \geq 0\}$. If $\partial\Omega \cap \rho^+_{(x_0,v)} \neq \emptyset$, we consider the reflection point

$$x_1 \in \partial\Omega \cap \rho^+_{(x_0,v)} : |x_0 - x_1| = \min_{y \in \partial\Omega \cap \rho^+_{(x_0,v)}} |x_0 - y|.$$

The perfect reflection is a pair (x_1, v_1) where x_1 is the point of reflexion and v_1 defines the reflected direction, ie., v_1 belongs to the plane defined by v_0 and the surface normal and makes the same angle with respect of normal direction as the incident direction defined by v_0.

We can define a map

$$\mathcal{R} : (\left(\mathbb{R}^D \backslash \Omega\right) \cup \{\infty\}, S^{D-1}) \to (\left(\mathbb{R}^D \backslash \Omega\right) \cup \{\infty\}, S^{D-1})$$

$$(x_0, v_0) \overset{\mathcal{R}}{\longmapsto} \begin{cases} (x_1, v_1) \quad if \ \partial\Omega \cap \rho^+_{(x_0,v)} \neq \emptyset, \\ (\infty, v_0) \ otherwise \end{cases} \tag{5.3}$$

$$(\infty, v) \longmapsto (\infty, v).$$

and iterate the map $\mathcal{R}$ starting with $x_0 \in \left(\mathbb{R}^D \backslash \bar{\Omega}\right)$ and $v_0 \in S^{D-1}$. This process defines a sequence (x_n, v_n) with $(x_n, v_n) = \mathcal{R}(x_{n-1}, v_{n-1}),\ n = 1, 2, ...$

Definition 3 We say that Ω is non trapping if the sequence (x_n, v_n) finishes at a fixed point, ie., $\exists n_0 \in \mathbb{N}$ such that $(x_n, v_n) = (\infty, v_{n_0}),\ \forall n \geq n_0$. Otherwise, we say that the domain is trapping (in this case, the sequence may oscillate between two values (x_1, v) and $(x_2, -v)$, as is illustrated in Fig. 1).

5.2 Distribution of the resonance frequencies

Now we will recall some classical results about the location of the resonance frequencies, depending on the geometry of the domain. In particular, they show that there is a clear difference between the distribution of resonance frequencies of trapping and

non trapping domains. The following result states that the resonance frequencies of a non trapping domain move away from the real axis, when their real parts increase (see [7]).

Theorem 3 *Let $\Omega \subset \mathbb{R}^3$ be a non trapping bounded domain with analytic boundary. Then, there exists $c > 0$ such that any resonance frequency μ satisfies*

$$Re(\mu) \leq -c\ |\mu|^{\frac{1}{3}}. \tag{5.4}$$

Moreover we have the following result [19].

Theorem 4 *Let $\Omega \subset \mathbb{R}^3$ be a non trapping domain. Then, for any $\alpha < 0$, the set*

$$\{z : 0 > Im(z) \geq \alpha\}$$

has, at most, a finite number of resonance frequencies.

In the opposite case, for the trapping case it is an open problem to prove/disprove the following conjecture (cf. [19, 21]).

Conjecture 1 *(Lax-Phillips) Let $\Omega \subset \mathbb{R}^3$ be a trapping domain. Then, there exists $\alpha < 0$, such that the set*

$$\{z : 0 > Im(z) \geq \alpha\}$$

has an infinite number of resonance frequencies.

The previous conjecture was already proved by Ikawa [16], in the particular case of a domain composed by two (or more) disjoint and convex domains.

In chapter 5 we will present some simulations for the distribution of the resonance frequencies of trapping and non trapping domains.

5.3 Numerical calculation of the resonances using the MFS

Again, we propose to consider the MFS with an auxiliary set of source points $y_1, ..., y_M \in \Gamma_M$, a family of points which is dense in $\gamma = \partial\omega$ and some random points $w_1, ..., w_R \in \omega$.

With the collocation points $x_1, ..., x_N \in \Gamma$ this leads to the matrix

$$\boldsymbol{M}(\kappa) = \begin{bmatrix} \Phi(|x_1 - y_1|) & \cdots & \Phi(|x_1 - y_M|) & \Phi(|x_1 - w_1|) & \cdots & \Phi(|x_1 - w_R|) \\ \vdots & \ddots & \vdots & \vdots & \ddots & \vdots \\ \Phi(|x_N - y_1|) & \cdots & \Phi(|x_N - y_M|) & \Phi(|x_N - w_1|) & \cdots & \Phi(|x_N - w_R|) \end{bmatrix} \tag{5.5}$$

which is a square matrix if $N = M + R$.

To obtain the resonance frequencies we might look for the $\kappa \in \mathbb{C}$ such that $\det(\boldsymbol{M}(\kappa)) = 0$. However, due to ill conditioning of the matrix $\boldsymbol{M}$, a more convenient approach is to use Betcke-Trefethen technique (cf. [9]). We consider a few random points $z_1, ..., z_P \in \mathbb{R}^D \backslash \bar{\Omega}$ and define the four-block matrix

$$\boldsymbol{A}(\kappa) = \left(\begin{array}{ccc|ccc} \Phi(|x_1-y_1|) & \cdots & \Phi(|x_1-y_M|) & \Phi(|x_1-w_1|) & \cdots & \Phi(|x_1-w_R|) \\ \vdots & \ddots & \vdots & \vdots & \ddots & \vdots \\ \Phi(|x_N-y_1|) & \cdots & \Phi(|x_N-y_M|) & \Phi(|x_N-w_1|) & \cdots & \Phi(|x_N-w_R|) \\ \hline \Phi(|z_1-y_1|) & \cdots & \Phi(|z_1-y_M|) & \Phi(|z_1-w_1|) & \cdots & \Phi(|z_1-w_R|) \\ \vdots & \ddots & \vdots & \vdots & \ddots & \vdots \\ \Phi(|z_P-y_1|) & \cdots & \Phi(|z_P-y_M|) & \Phi(|z_P-w_1|) & \cdots & \Phi(|z_P-w_R|) \end{array}\right). \tag{5.6}$$

Then, we calculate the **QR** decomposition of matrix $\boldsymbol{A}(\kappa)$,

$$\boldsymbol{A}(\kappa) = \begin{pmatrix} \boldsymbol{Q}_\Gamma(\kappa) \\ \boldsymbol{Q}_{\mathbb{R}^D\backslash\Omega}(\kappa) \end{pmatrix} \boldsymbol{R}(\kappa)$$

and study the evolution of smallest singular value of the matrix $\boldsymbol{Q}_\Gamma(\kappa)$, that we denote by $\sigma_1(\boldsymbol{Q}_\Gamma(\kappa))$. The approximations of the resonance frequencies are the values κ for which $\sigma_1(\boldsymbol{Q}_\Gamma(\kappa)) \approx 0$.

6 Numerical experiments

We start by considering the case of the unitary disk and the source points are placed on a circumference centered at the origin and radius equal to 0.8, taking $N = M = 50$ and $R = 0$, that is, considering just point sources on γ (and not in ω). Figure 2 show the plot of the map $\kappa \mapsto \log(|\det(\boldsymbol{M}(\kappa))|)$. We mark with dashed red lines the eigenfrequencies of the interior Dirichlet eigenvalue problem defined in ω. As expected from our previous discussion, the matrix $\boldsymbol{M}(\kappa)$ is singular, when κ coincides with one of those eigenfrequencies.

Next, we test the approach that we described in previous section, by studying the evolution of $\sigma_1(\boldsymbol{A}(\kappa))$. We show an illustrative example for κ in an interval containing the second Dirichlet eigenfrequency of the interior eigenvalue problem in ω. We will consider three different situations that are illustrated in the first row of plots of Fig. 3. In both cases we take 100 collocation points on Γ (marked with $\circ$), 10 random points in $\mathbb{R}^2\backslash\bar{\Omega}$ (marked with $*$) and 50 source points marked with $\bullet$. In the first case (left plot) all the source points are located on γ, in the second case we take 40 source points on γ and 10 on an axis of symmetry of the disk (center plot) and finally in the last case we take 40 source points on γ and 10 random points in ω. The second row of pictures show the corresponding graphs of $\sigma_1(\boldsymbol{A}(\kappa))$. The second eigenfrequency of the interior problem in ω is marked with a dashed red line. We can observe that in the first two cases, the plot presents an oscillation close to this spurious eigenfrequency. Since our

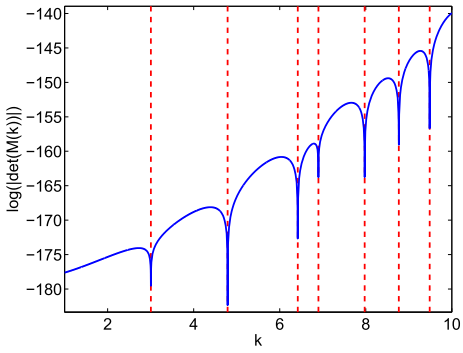

Fig. 2 Plot of the map $\kappa \mapsto \log(|\det(\boldsymbol{M}(\kappa))|)$, for $\kappa \in [1, 10]$. The eigenfrequencies of the interior problem defined in ω are marked with dashed red lines

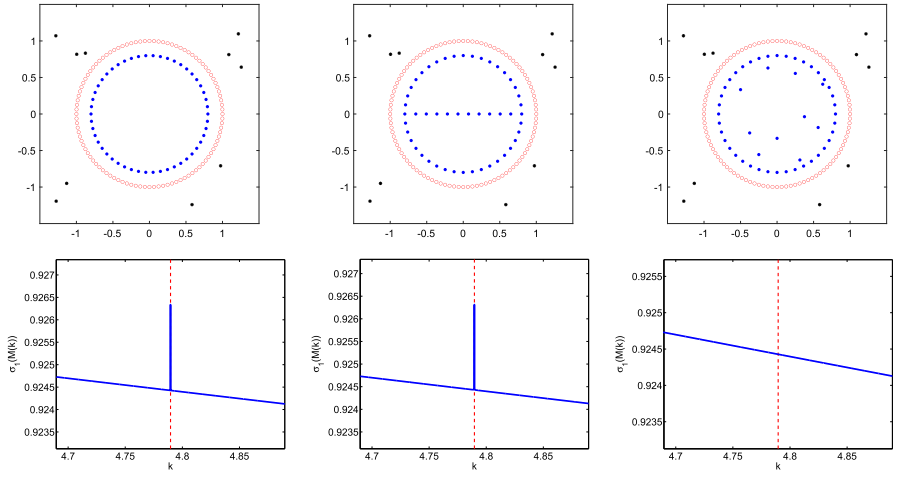

Fig. 3 Three choices of the source points and the corresponding plots of $\sigma_1(\boldsymbol{A}(\kappa))$. In the first two cases we have an oscillation due to the existence of a spurious eigenfrequency

numerical algorithm for the calculation of the resonances depend on the study of the evolution of $\sigma_1(\boldsymbol{A}(\kappa))$, these oscillations can lead to difficulties, especially if for the range of frequencies κ considered we have $\sigma_1(\boldsymbol{A}(\kappa))$ close to zero. In the last case, the oscillation has disappeared. Note that in the second case, the source points placed in ω are located on a nodal line of the eigenfunction. Thus, this choice is not effective to remove the effect of the spurious eigenfrequency and we need to consider a healthier choice of the points, for instance placing them randomly in ω, as was considered in the last case.

Next, we consider a slight perturbation of the source points plotted in the middle picture of Fig. 3. Instead of placing points on the line defined by $y = 0$, we define the second component of the points to be obtained as realizations of a random variable $Y = 10^{-6}Z$, where Z follows a standard normal distribution, as shown in the middle picture of Fig. 4. The oscillation due to the existence of a spurious eigenfrequency that was shown in Fig. 3 is not observed at this scale with this perturbed location of the source points.

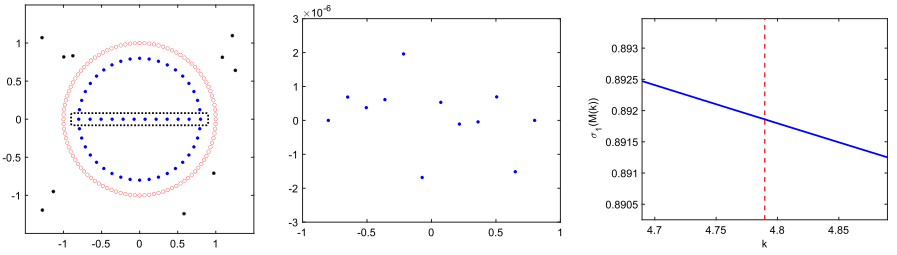

Fig. 4 Plot of the location of the source points (left picture); zoom of the region close to the line $y = 0$, showing the source points close to the line define by $y = 0$ (middle picture); plot of $\sigma_1(\boldsymbol{A}(\kappa))$ (right plot). The oscillation due to the existence of a spurious eigenfrequency that was shown in Fig. 3 is not observed at this scale with this perturbed location of the source points

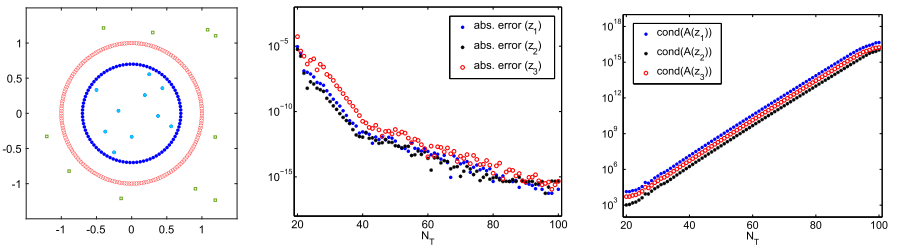

Fig. 5 Convergence and conditioning results for three resonance frequencies of the unit disk

Next, we test the convergence of the numerical method in the case of the unit disk with the setting of points presented in Fig. 5-left. We took $P = 10$ random points $z_1, ..., z_{10} \in \mathbb{R}^2 \backslash \Omega$ marked with the symbol $\square$, $R = 10$ interior source points generated with a Halton distribution marked with $\bullet$, M source points on a circumference centered at the origin and radius equal to 0.7, represented with the symbol $\bullet$ and will denote by N_T the total number of source points. Finally, we took $2N_T$ collocation points on the boundary that are marked with $\circ$. We will show some convergence results for three resonance frequencies

$$
\begin{aligned}
z_1 &= -0.419274604094181 - 0.577399524117206i \\
z_2 &= -3.83244286765062 - 0.354904706219262i \\
z_3 &= -1.31684116739175 - 0.836104483291729i .
\end{aligned}
$$

Figure 5 shows the absolute error of the numerical approximations for the three resonance frequencies, as a function of N_T. The right plot of the same figure shows the condition number of the matrices $\boldsymbol{A}(z_i)$, $i = 1, 2, 3$, as a function of N_T. The method allows to achieve a double precision accuracy but the condition number grows exponentially.

Next, we apply the numerical method in an example of a non trapping 2D domain whose boundary can be parameterized by

$$
\partial\Omega = \left\{ \left(1 + \frac{1}{4}\cos(3t) \right) (\cos(t), \sin(t)) : t \in [0, 2\pi[\right\} .
$$

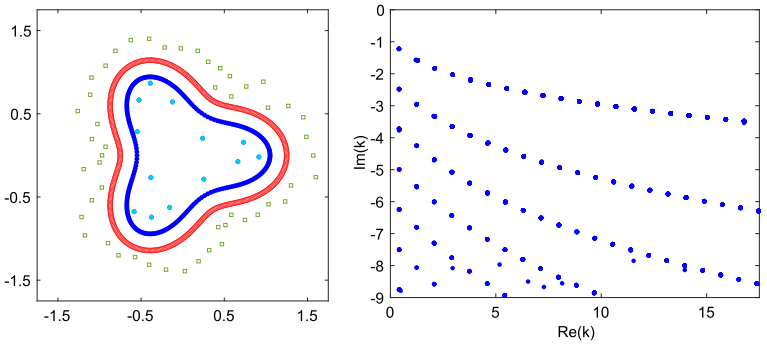

Fig. 6 The points considered in a non trapping 2d domain (left plot) and the distribution of the resonance frequencies

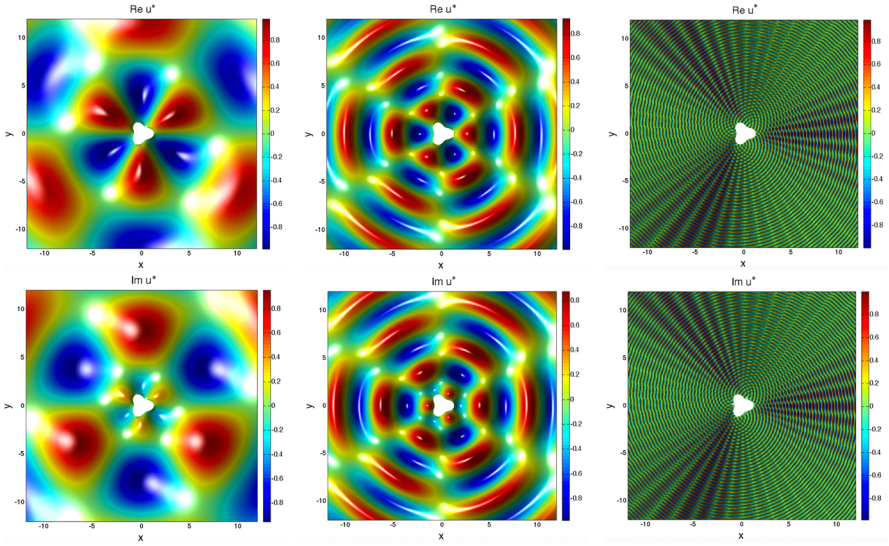

Fig. 7 Plots of the real and imaginary parts of the functions u^* of a 2D non trapping obstacle, for three resonance frequencies $\kappa_1 = -0.3990505 - 1.8223030i$, $\kappa_2 = 1.29547456 - 1.5835340i$ and $\kappa_3 = 18.5238690 - 3.5908771i$

The left plot of Fig. 6 shows the points considered for the calculation of the resonance frequencies, whose distribution in the complex plane is presented in the right plot of the same figure. We can observe that there is a resonance free region close to the real axis and the imaginary parts of the resonance frequencies move away from the real axis.

Figure 7 shows the plots of the real and imaginary parts of the function $u^* := \dfrac{u}{e^{-i\kappa_I r}}$ for three resonance frequencies $\kappa_1 = -0.3990505 - 1.8223030i$, $\kappa_2 = 1.29547456 - 1.5835340i$ and $\kappa_3 = 18.5238690 - 3.5908771i$.

Next, we consider a 2D trapping domain shown in left plot of Fig. 8. In the right plot of the same Figure we represent the resonance frequencies. In this case, since we

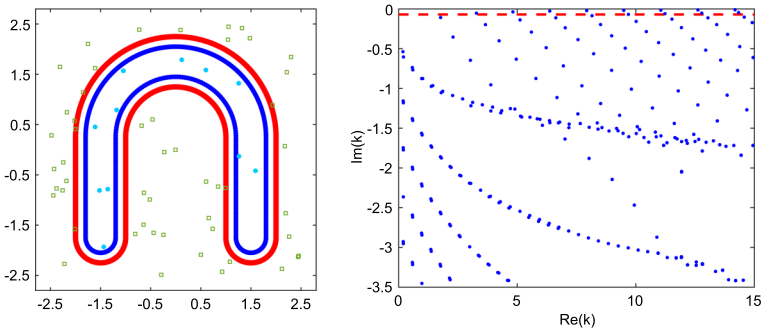

Fig. 8 The points considered in a 2D trapping obstacle (left plot) and the distribution of the resonance frequencies which suggest that for any $\epsilon > 0$, we may have some resonance frequencies verifying $Im(\kappa) > -\epsilon$.

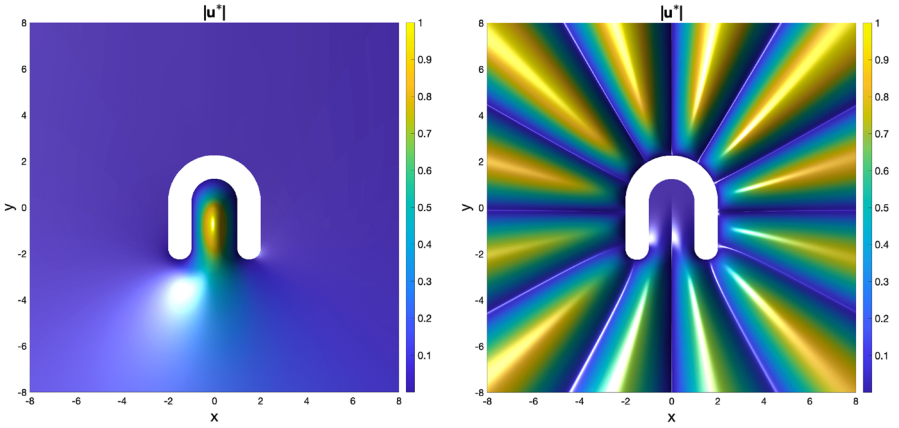

Fig. 9 Plots of $|u^*|$ for two resonance frequencies $\kappa_1 = 1.7679092 - 0.1077933i$ and $\kappa_2 = 1.7935326 - 1.0533207i$. The resonance frequencies have approximately the same real part, but κ_1 is much closer to the real axis than κ_2. The function u^* associated to κ_1 is localized in the trapping region

have a trapping obstacle, we can observe that some frequencies approach the real axis. Indeed, the results suggest that for any arbitrarily small value $\epsilon > 0$, there are always some resonance frequencies verifying $Im(\kappa) > -\epsilon$, as illustrated in the right plot of Fig. 8.

Figure 9 shows the plot of $|u^*|$ for two resonance frequencies $\kappa_1 = 1.7679092 - 0.1077933i$ and $\kappa_2 = 1.7935326 - 1.0533207i$ of the 2D trapping obstacle represented in the left plot of Fig. 8. The resonance frequencies have approximately the same real part but κ_1 is close to the real axis, while the κ_2 is not so close. We can observe that in the first case, the function u^* is localized in the trapping region, while in the second the function u^* is not localized.

Next, we test the numerical method in two examples of 3D obstacles. In the first example we consider the 3D unitary ball and consider the points represented in the left plot of Fig. 10. In the right plot of the same figure we plot the distribution of the approximate resonance frequencies together with the exact values, directly obtained by

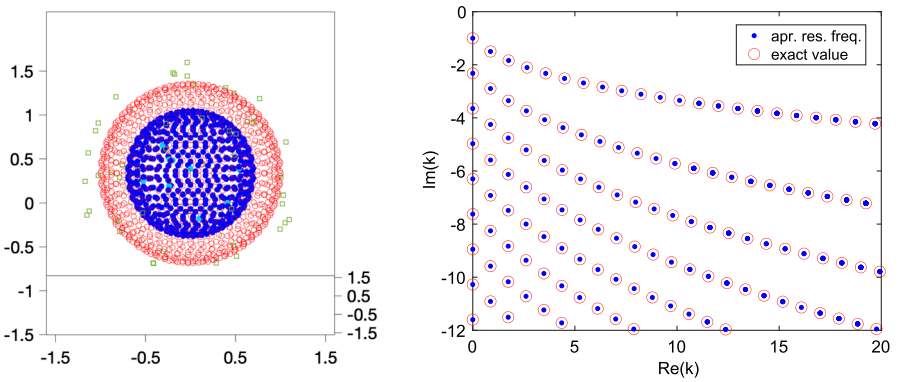

Fig. 10 The points for the numerical method in the case of the unitary 3D ball (left plot) and the distribution of the resonance frequencies. We plot the approximate resonance frequencies and also the corresponding exact values

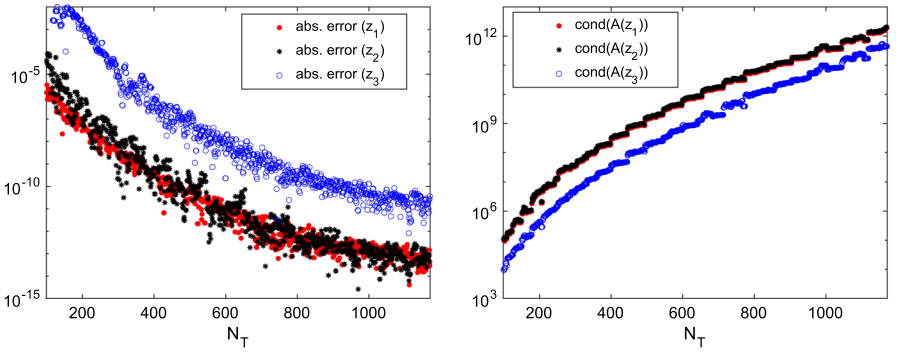

Fig. 11 Plot of the absolute errors of three resonance frequencies, as a function of the number of MFS source points, N_T (left plot) and plot of the condition numbers of the matrix $\mathbf{A}$

calculating zeros of Hankel functions. Figure 11 shows convergence and conditioning results for three resonance frequencies

$$
\begin{aligned}
z_1 &= -i \\
z_2 &= 1.75438095978372 - 1.83890732268696i \\
z_3 &= 8.23269945907359 - 3.1089162336491i.
\end{aligned}
$$

Finally, we consider an example of a 3D trapping domain for which we consider the points plotted in Fig. 12. The resonance frequencies are represented in the right plot of the same figure. Again we can find some resonance frequencies approaching the real axis.

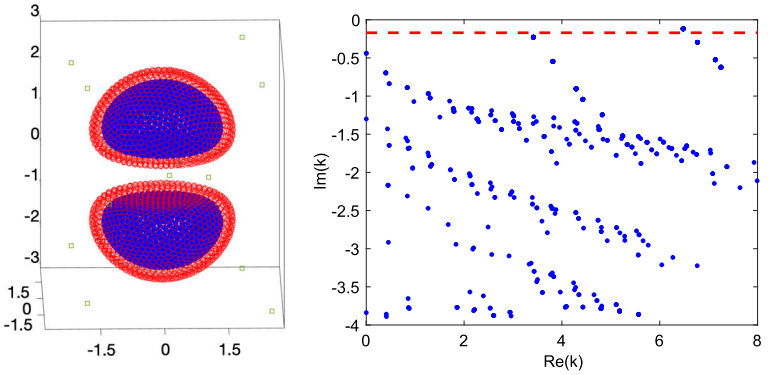

Fig. 12 Points for the numerical method in the case of 3D trapping domain (left plot) and the distribution of the resonance frequencies in the complex plane. Some of them approach the real axis

7 Conclusions

We proved density and convergence results supporting the application of the method of fundamental solutions for solving wave scattering problems in exterior domains. Several numerical simulations illustrate the good performance of the method in the calculation of resonance frequencies in trapping and non trapping domains in 2D and 3D.

Acknowledgements We would like to thank the anonymous referee for many suggestions and comments that clearly improved the quality of the paper.

Funding Open access funding provided by FCT|FCCN (b-on).

References

1. Albert, J.H.: Genericity of simple eigenvalues for elliptic PDE s. Proc. Amer. Math. Soc. **48**, 413–418 (1975)
2. Alves, C.J.S.: On the choice of source points in the method of fundamental solutions. Eng. Anal. Bound. Elem. **33**, 1348–1361 (2009)
3. Alves, C.J.S.: Numerical simulations on resonance poles - the trapping case of two plane cracks. J. Comput. Appl. Math. **111**, 267–279 (1999)
4. Alves, C.J.S., Antunes, P.R.S.: The method of fundamental solutions applied to some inverse eigenproblems. SIAM J. Sci. Comp. **35**, A1689–A1708 (2013)
5. Antunes, P.R.S.: A numerical algorithm to reduce ill-conditioning in meshless methods for the Helmholtz equation. Numer. Algorithms **79**(3), 879–897 (2018)

6. Bardos, C., Guillot, J.C., Ralston, J.: La relation de Poisson pour l'équation des ondes dans un ouvert non borné. Application à la théorie de la diffusion. Comm. Part. Differ. Equ. **7**, 905–958 (1982)
7. Bardos, C., Lebeau, G., Rauch, J.: Scattering frequencies and Gevrey 3 singularities. Invent. Math. **90**, 77–114 (1987)
8. Barnett, A.H., Betcke, T.: Stability and convergence of the method of fundamental solutions for Helmholtz problems on analytic domains. J. Comput. Phys. **227**(14), 7003–26 (2008)
9. Betcke, T., Trefethen, L.N.: Revining the method of particular solutions. SIAM Rev. **47**(3), 469–491 (2005)
10. Bogomolny, A.: Fundamental solutions method for elliptic boundary value problems. SIAM J. Numer. Anal. **22**(4), 644–669 (1985)
11. Burton, A.J., Miller, G.F.: The application of integral equation methods to numerical solution of some exterior boundary value problems. Proc. R. Soc. Lond. A **323**, 201–210 (1971)
12. Chen, I.L., Chen, J.T., Liang, M.T.: Analytical study and numerical experiments for radiation and scattering problems using the CHIEF method. J. Sound Vib. **248**, 809–828 (2001)
13. Chen, J.T., Chen, I.L., Lee, Y.T.: Eigensolutions of mutiply connected membranes using the method of fundamental solutions. Eng. Anal. Bound. Elem. **29**, 166–174 (2005)
14. Colton, D., Kress, R.: Inverse Acoustic and Electromagnetic Scattering Theory. Springer-Verlag, Berlin (2012)
15. Fairweather, G., Karageorghis, A., Martin, P.A.: The method of fundamental solutions for scattering and radiation problems. Eng. Anal. Bound. Elem. **27**, 759–769 (2003)
16. Ikawa, M.: On the poles of the scattering matrix for two strictly convex obstacles. J. Math. Kyoto Univ. **23**, 127–194 (1983)
17. Jones, D.S.: Integral equations for the exterior acoustic problem. Q. J. Mech. Appl. Math. **XXVII**, 129–142 (1974)
18. Kupradze, V.D., Aleksidze, M.A.: The method of functional equations for the approximate solution of certain boundary value problems. Comput. Math. Math. Phys. **4**, 82–126 (1964)
19. Lax, P., Phillips, R.: Scattering Theory: Pure and Applied Mathematics. Academic Press, Cambridge (1967)
20. Lax, P., Phillips, R.: A logarithmic bound on the location of the poles of the scattering matrix. Arch. Rat. Mech. Anal. **40**, 268–280 (1971)
21. Melrose, R.B.: Geometric Scattering Theory. Cambridge University Press, Cambridge (1995)
22. Micheletti, A.M.: Perturbazione dello spettro di un operatore ellittico di tipo variazionale, in relazione ad una variazione del campo. Ann. Scuola Norm. Sup. Pisa **26**, 151–169 (1972)
23. Morawetz, C.S., Ralston, J.V., Strauss, W.: Decay of the solutions of the wave equation outside non-trapping obstacles. Commun. Pure Appl. Math. **30**, 447–508 (1977)
24. Panich, O.: On the question of solvability of the exterior boundary-value problems for wave and Maxwell's equations. Usp. Mat. Nauk. **20A**, 221–226 (1965). (**(in Russian)**)
25. Poisson, O.: Étude numérique des pôles de résonance associés à la diffraction d'ondes acoustiques et élastiques par un obstacle en dimension 2. Math. Modell. Numer. Anal. **29**, 819–855 (1995)
26. Schenck, H.A.: Improved integral formulation for acoustic radiation problem. J. Acoust. Soc. Am. **44**, 41–58 (1968)
27. Seybert, A.F., Rengarajan, T.K.: The use of CHIEF to obtain unique solutions for acoustic radiation using boundary integral equations. J. Acoust. Soc. Am. **81**, 1299–1306 (1987)
28. Uhlenbeck, K.: Generic properties of eigenfunctions. Am. J. Math. **98**(4), 1059–1078 (1976)
29. Zhang, L.-P., Li, Z.-C., Huang, H.-T., Lee, M.-G.: Comparisons of method of fundamental solutions, method of particular solutions and the MFS-QR; stability analysis. Eng. Anal. Bound. Elem. **123**, 182–199 (2021)